J Mater Sci: Mater Med (2011) 22:339–347
DOI 10.1007/s10856-010-4196-0

Bio-inspired porous SiC ceramics loaded with vancomycin for preventing MRSA infections

P. Díaz-Rodríguez · M. Landin · A. Rey-Rico · J. Couceiro · T. Coenye · P. González · J. Serra · M. López-Álvarez · B. León

Received: 21 May 2010 / Accepted: 24 November 2010 / Published online: 5 December 2010

Abstract Implant-related infections are a serious complication in orthopaedic and dental surgery resulting in prolonged hospitalization, high medical costs and patient mortality. The development of porous implants loaded with antibiotics may enable a local delivery for preventing surface colonization and biofilm formation. A new generation of bio-derived porous ceramic material that mimics hierarchical structures from Nature was evaluated. Silicon carbide ceramics derived from Sapelli wood (bioSiC) were obtained by pyrolysis of *Entandrophragma cylindricum* wood followed by infiltration with molten silicon. This process renders disks that keep the bimodal pore size distribution (3 and 85 μm) of the original material and are highly cytocompatible (BALB/3T3 cell line). The ability of the bio-ceramic to load the antimicrobial agent vancomycin was evaluated by immersion of disks in drug solutions covering a wide range of concentrations. The disks released at pH 7.4 an important amount of drug during the first 2 h (up to 11 mg/g bioSiC) followed by a slower release, which is related to the presence of macro- and mesopores. Finally, the anti-biofilm effect against methicillin resistant *Staphylococcus aureus* was assessed and a considerable reduction (92%) of the bacterial film was observed. Results highlight the bioSiC potential as component of medicated medical devices.

P. Díaz-Rodríguez · M. Landin (✉) · A. Rey-Rico
Dpto. Farmacia y Tecnología Farmacéutica, Facultad de Farmacia, Universidad de Santiago de Compostela, 15782 Santiago de Compostela, Spain
e-mail: m.landin@usc.es

J. Couceiro
Inst. de Ortopedia y Banco de Tejidos Musculoesqueléticos, Universidad de Santiago de Compostela, Santiago de Compostela, Spain

T. Coenye
Laboratorium voor Farmaceutische Microbiologie, Universiteit Gent, Ghent, Belgium

P. González · J. Serra · M. López-Álvarez · B. León
Dpto. Física Aplicada, E.T.S.E. Industriais, Universidade de Vigo, Vigo, Spain

1 Introduction

After roughly 100 years of clinical use of ceramics in dentistry and orthopaedics, there is still a need for novel biomaterials. Chevalier and Gremillard [1], in their recent and extensive review on ceramics for medical applications, stated the imperative need for obtaining novel, tough and stable materials (with special mention to non-oxide ceramics as silicon carbide or silicon nitride) as orthopedic material candidates. Additionally, these authors pointed out the interest of developing those new materials through a biomimetic approach. Huebsch and Mooney [2] emphasize that there is a considerable body of research on the importance of physical variables, including topological and mechanical properties of biomaterials, in guiding a biological response. Some materials originated from living organisms, as bones, have outstanding properties due to their inorganic nature but also to their complex structural organization. To achieve a synthetic material that matches to bone, one has to take care of both these aspects. Bones are made up of a collection of materials built out of a common basic building block, the mineralized collagen fibril, that can be arranged in different patterns. All forms of bone possess mechanical strength and toughness out of reach from its constituent materials [3]. Numerous attempts have been made to mimic the structure of bone [4–6]. Highly porous calcium phosphate ceramic scaffolds or

organic–inorganic composites are well known examples that have been used successfully [7], but none of them simultaneously combined the microscopic and macroscopic structure of the bone. Mimicking bone structure continues to be a challenging task.

Bio-derived silicon carbide based ceramics (bioSiC), obtained by Si-melt infiltration of carbonaceous scaffolds derived from wood templates have been proposed as new engineering ceramic materials with potential use in biomedical applications [8, 9]. As a result of the evolution, wood combines a good balance between resistance/weight ratio and fluids circulation. BioSiC are non-oxide ceramics that keep the complex natural structural organization of wood, resembling to a certain extent that of bones. Biocompatible bioSiC can be produced with low cost, near-net-shape and adequate mechanical properties [8–10]. The possibility of varying the wood cellulosic preforms and/or the process variables makes the bioSiC approach extremely versatile and allows to tailor microstructures resulting in materials with different densities, morphologies, pore size distributions, levels of anisotropy, mechanical strength, etc. [8] and, thus, potentially useful as candidates for the development of orthopedic and dental implants.

Bone infections are typically caused by bacteria introduced from trauma, surgery, implant use, or by direct colonization from a proximal infection or via systemic circulation. Postoperative osteomyelitis is still an important problem in orthopedic and dental surgery [11]. The bacterial biofilm, extremely resistant to both the immune system and antibiotics, is considered the primary cause of implant-associated infection. During the first 6 h after surgery, an implant is particularly susceptible to surface colonization and biofilm formation [11]. Efficiency of the systemic treatment of osteomyelitis is limited by the difficult access of the antibiotic to the infection site [12, 13]. The use of implants loaded with antimicrobial agents is a promising approach to prevent post-operative infections [14]. The effectiveness of the antibiotic/device combinations is strongly dependent on the mechanism and the rate of drug release [15]. Sub-inhibitory drug concentrations (i.e., those below the minimal inhibitory concentration) does not prevent the formation of a microbial biofilm and may even exacerbate complications or induce resistance in wound-site bacteria. An initial "burst" release from the device may sufficiently reduce the likelihood of the primary biofilm infection and, as a consequence, improve the prophylaxis against infection and speed-up the patients recovery. Recent studies have demonstrated that microporous materials may be particularly useful as drug-eluting implants. Porous hydroxyapatite enables more absorption and longer antibacterial activity (up to 2 days) in vitro than dense hydroxyapatite (only 12 h) [16]. On the other hand, mesoporous silica with a highly regular nano-porous structure and a vast surface area provided controlled release and an excellent protection for the loaded guest molecules [17].

The aim of the present work was to evaluate the potential of a bioSiC from Sapelli wood for the loading and the release of vancomycin in order to prevent local bacterial infections, including biofilms formed by methicillin resistant *Staphylococcus aureus* (MRSA). To the best of our knowledge the suitability of bioSiC as drug delivery system has not been evaluated yet. Vancomycin is a highly soluble (>100 mg/ml) antimicrobial agent, which is usually administered systemically after bone surgery to prevent bacterial infection because of its broad spectrum and particular efficiency against staphylococci [18, 19]. First, the porosity and topography of the bioSiC was characterized in detail in order to confirm the mimicking of the smart hierarchical structure of the tree template. Cytocompatibility and cell conductive properties were then tested. Finally, the ability of bioSiC to load vancomycin and to prevent the biofilm formation was evaluated and related to the particular hierarchical structure of the disks.

2 Materials and methods

2.1 Bio-inspired silicon carbide

Pieces of bioSiC were obtained from transversal cuts of Sapelli wood (*Entandrophragma cylindricum).* The bioceramization process consisted of drying the wood at 60°C for 24 h, after which pieces were subjected to pyrolysis up to 800°C in an inert atmosphere with well controlled heating and cooling ramps. Finally, the carbon preform obtained was infiltrated with molten silicon at 1,550°C in vacuum for 30 min [9]. The final material was cut to obtain disks of Ø 6 mm × 2 mm.

2.2 BioSiC characterization

The microstructure and topography of bioSiC disks were evaluated by Scanning Electron Microscopy (SEM Philips XL 30), Interferometric Profilometry (WYKO NT-1100) and Confocal Laser Scanning Microscopy (CLSM Bio-Rad MRC 1024). The material density was determined, by triplicate, using a helium-air pycnometer (Quantacrome Mod. PY2, USA). The pore size distribution was evaluated by mercury intrusion porosimetry using a Micromeritics Autopore IV 9500 (Norcross, GA, USA) fitted with a 3-ml penetrometer for solids. The working pressures covered the range 0.6–2.5 × 10^4 psi. The specific surface area was evaluated by the Brunauer–Emmett–Teller (BET) method [20] which involved the determination of the amount of the adsorptive gas (N_2 in this case) required to cover the

external and the accessible internal pore surface of the material with a complete monolayer. The disks were degassed by heating at 60°C and 10^{-3} mm Hg. Then, samples were exposed to N_2 gas at 77 K and 0.01–0.98 relative pressure on an automatic surface area analyzer (Micromeritics ASAP 2000, USA). The BET surface area (S_{BET}) was calculated from the isotherms according to the BET equation: S_{BET} (m^2 g^{-1}) = 4.37 V_m (cm^3 g^{-1}), where V_m is the volume of nitrogen necessary to form the monolayer.

2.3 Cell viability test

The in vitro cytocompatibility of bioSiC disks was tested, in triplicate, by using a BALB/3T3 cell line (CCL 163, ATCC, USA), according to the 10993-5 protocol of the International Standardization Organization (ISO). A cell suspension of 200,000 cells/well in 2 ml of DMEM (GIBCO^{TM}), supplemented with 10% fetal bovine serum (FBS) and 1% gentamicine, was added into a 24-well plate. Then bioSiC disks were placed in the wells and the plate was incubated at 37°C for 24 h in 5% of CO_2 and 90% of relative humidity environment. A control (cells without bioSiC disk) was treated in the same way. The bioSiC samples were collected and dyed in order to assess live/dead populations by means of a calcein/propidium iodide staining using confocal microscopy (Confocal Spectral Microscopy Leica TCS-SP2 LEICA, Wetzlar, Germany). To calculate their ratio (viability), live and dead populations were counted by using a light microscope (Optiphot2, Nikon, Japan) with green and red filters and Image Analysis software (Soft Imaging System GmbH, Version 3.2 Build 0.607). Cells remaining adhered to the tissue culture polystyrene (TCP) well were trypsinized and centrifuged. The pellet was resuspended with cell culture medium, cytospinned onto a glass slide, and dyed with calcein and propidium iodide.

2.4 Vancomycin loading

The high solubility in water of vancomycin enabled the loading of this antimicrobial agent into bioSiC disks by a simple immersion in 3 ml of drug aqueous solutions with concentrations ranging from 0.05 to 42.5 mg/ml. The disks were left in the drug solution for 24 h with mechanical shaking. Vacuum (75 mm Hg) was applied for the first 2 h to eliminate the air from the pores of the pieces and to promote the flux of drug solution into the disks. The amount of vancomycin loaded in each disk was calculated as the difference between the initial and the final concentrations in the surrounding solution, determined by UV spectrophotometry at 280 nm (Agilent 8453, Böblingen, Germany). All the experiments were carried out in duplicate. Drug-loaded disks were desiccated at 40°C until constant weight. BioSiC material loaded with vancomycin was evaluated as it was indicated above.

2.5 Vancomycin release

Dried drug-loaded disks were transferred to vials containing 3 ml of phosphate buffer (PBS) pH 7.4 at 37°C and kept under mechanical shaking. Samples of the release medium were withdrawn at regular intervals and returned to the vial immediately after their drug concentration was measured spectrophotometrically at 280 nm. Water uptake by the disks was monitored in parallel to the release tests by placing of dried disks in a Gay-Lussac pycnometer (Afora, Spain) and weighing the pycnometer at different times after filling with water.

2.6 MRSA biofilm formation

BioSiC material and vancomycin-loaded bioSiC disks, prepared by immersion in 42.5 mg/ml of drug solution during 24 h, were subjected to this microbiological study by using a clinical MRSA isolate. This bacterial isolate (recovered from a patient at the Ghent University Hospital, Ghent, Belgium) was grown on Tryptic Soy Agar (TSA) (Oxoid, Drongen, Belgium) at 37°C. MRSA biofilms were formed in two different model systems. First, MRSA biofilms were formed in the Modified Robbins Devices (MRD), as described previously [21]. In this system, growth medium is continuously replaced. Secondly, biofilms were formed on drug loaded-bioSiC disks using 24-well microtiter plates (MTP, Trasadingen, Switzerland). To this end, disks were placed in 1 ml MRSA suspensions with a density of appr. 10^6 CFU/ml (in 1:5 diluted Tryptic Soy Broth, TSB) for 1 h. Subsequently, disks were gently rinsed with 0.9% (w/v) NaCl to remove non-adherent cells and were placed in 1 ml diluted TSB for an additional 24 h at 37°C. To quantify the biofilm formation in both methods the MRD and MTP, each disk was transferred to test tubes with 10 ml 0.9% (v/w) NaCl and the tubes were subjected three times to 30 s of sonication (Branson 3510, 42 kHz, 100 W, Branson Ultrasonics Corp., Danbury, USA) and 30 s of vortex mixing to detach the biofilm from the disks. Using this procedure all cells were removed from the disks and clumps of cells were broken apart. Sessile *S. aureus* cells were platted on TSA, and incubated at 37°C for 48 h. Finally, the number of colony forming units (CFU) per disk was calculated by counting colonies on the plates. All experiments were carried out on at least 3 disks for each composition. The Student *t* test was used to evaluate the efficacy in reducing cell colonies and the differences between MRD and MTP methods.

3 Results

Processing variables during bioSiC production may affect the interconnected microstructure of the wood template. Morphological characterization of bioSiC was carried out by SEM micrographs (Fig. 1) that evidenced the particular porous microstructure of the Sapelli tree. Macropores ($\sim$80 μm) in groups of two or three, characteristic of the Sapelli tree (A), can be seen at the surface of the cross section of bioSiC. More in detail (B) a second population of mesopores (less than 10 μm) at the surface of the material can be noticed, with the silicium carbide crystals making the structure up (C). The walls of the vessels were maintained after infiltration giving a ceramic material with pores unidirectional connected, as it can be noted at the longitudinal section (Fig. 2) characterized by interferometric profilometry (A) and confocal laser scanning microscopy (B).

Microstructure was also confirmed from mercury intrusion porosimetry measurements (Fig. 2). Results evidence a total intrusion volume was 0.243 ± 0.005 ml/g and a total porosity of $41.49 \pm 0.05\%$ with a bimodal pore size distribution (Fig. 3) including macropores (mean diameter $\simeq$ 85 μm) and mesopores (mean diameter $\simeq$ 3 μm). Quantitative differences in the micro structural properties between vancomycin loaded and unloaded bioSiC disks could not be established using mercury intrusion porosimetry.

The nitrogen adsorption analysis confirmed the absence of microporosity and allowed the estimation of specific surface (1.198 ± 0.005 m^2 g^{-1}).

The ability of bioSiC disks to sustain cell attachment and growth was assessed by an in vitro biocompatibility test following ISO 10993-5 procedure. The assays were conducted using Balb cell line. After 24 h in contact, a homogeneous well distributed layer of living cells and a significantly smaller amount of dead cells on the top of the bioSiC disks can be observed (Fig. 4). The ratio between living and dead cells was used to calculate the viability of cells on the disk. The obtained values were 79.9% (sd 13.1) on bioSiC disks, 98.0% (sd 1.9) on the TCP from the wells and 86.2% (sd 15.3) for the control group. Vancomycin loaded bioSiC were also tested to assure in vitro biocompatibility achieving a percentage of viability of 95.8% (sd 6.0).

Figure 5 shows the adsorption curve of vancomycin on bioSiC material which relates the concentration of the solute on the adsorbent (mg vancomycin per gram of dried material) to the concentration of the solute in the surrounding solution at the equilibrium. The shape of the adsorption curve can be classified as Class S according to Giles and coworker classification [22]. At the highest loading concentration studied (6 mg/ml) a significant amount of vancomycin (nearly 50 mg/g of bioSiC) was loaded.

When the loaded disks were immersed in 3 ml phosphate buffer pH 7.4 in order to simulate the release process under body conditions, a rapid delivery occurred during the first 2 h (Fig. 6) followed by a slower rate after. Figure 6 shows the profiles for the first hours (critical period after surgery) but the antibiotic release slowly continues for weeks. The total amounts released in the first 2 h are significantly lower but proportional to the adsorbed vancomycin estimated from the adsorption experiments.

Finally, the effectiveness of bioSiC disks loaded by immersion in 42.5 mg/ml vancomycin solution to prevent MRSA biofilm formation was tested in two model systems, one (the MRD) in which the growth medium was continuously replaced and another one (the MTP) in which growth medium was not replaced. In the MRD, unloaded control disks contained on, average 6.76×10^4 CFU/disk while vancomycin-containing disks contained 4.57×10^4 CFU/disk (a reduction of 31.4%) (Fig. 7) but the difference was not statistically significant. On the contrary, the antibiofilm effect in the MTP was much more pronounced and statistically significant ($t = 3.45$; 5 and 7 df $\alpha < 0.05$), with control disks containing 1.10×10^4 CFU/disk and the vancomycin-containing disks only contained 5.50×10^2 CFU/disk (a reduction of 94.99%). Data indicate that vancomycin is being released in both model systems.

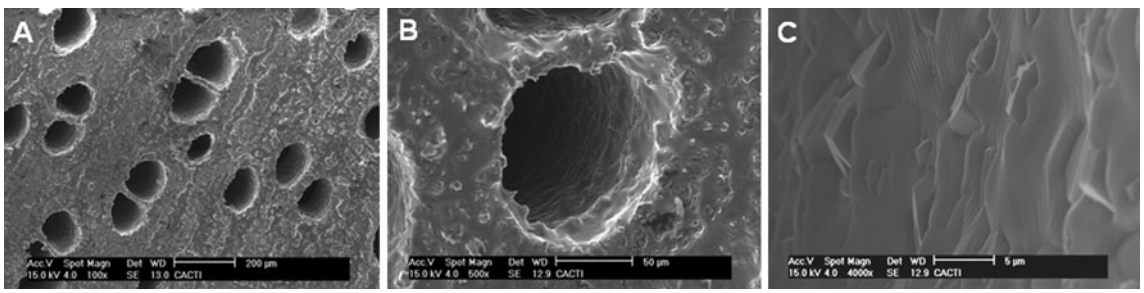

Fig. 1 SEM micrographs (cross-section) of bioSiC ceramics produced from Sapelli wood. Three magnifications are shown: **a** (×100), **b** (×500) and **c** (×4,000)

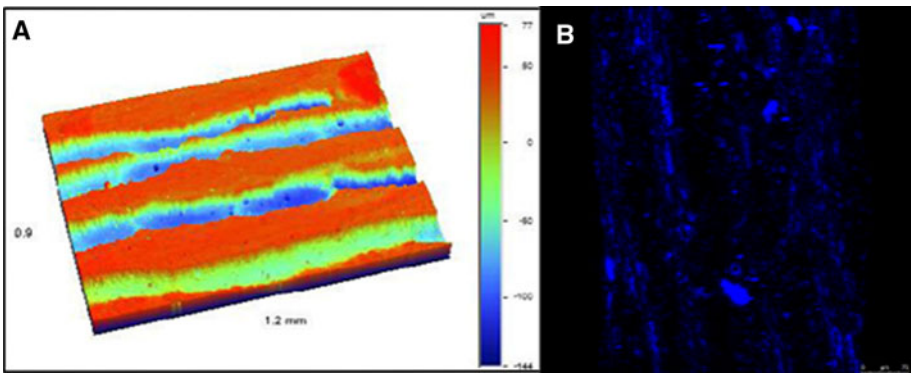

Fig. 2 Topographic characteristics of a bioSiC ceramic (longitudinal section) by interferometric profilometry (**a**) and confocal laser scanning microscopy (**b**)

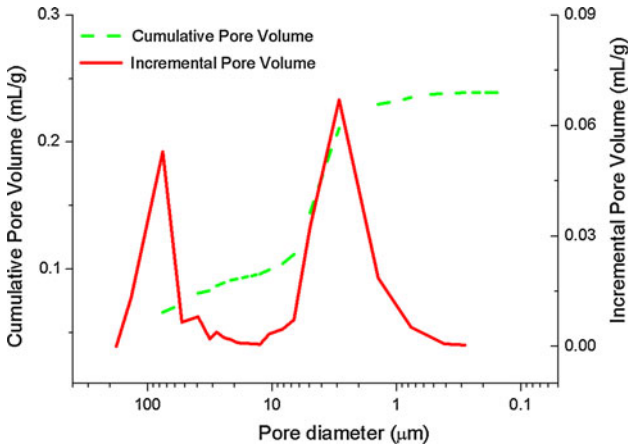

Fig. 3 Pore size distribution and percentage of porosity of bioSiC derived from Sapelli wood

4 Discussion

As a hardwood, Sapelli wood microstructure includes three types of pores: vessels which are large cells to transport nutrients, and fibers and rays, which are smaller in diameter cells used for strength and storage [23]. The vessels and fibers are elongated and run in the axial (longitudinal) direction of the tree. The rays are aligned perpendicularly to the vessels and fibers, in the transverse direction [24]. The microstructure and the density of Sapelli wood are particularly appealing for its use as scaffold molds, while the mechanical properties of the wood can be remarkably improved by a rapid and controlled mineralization. The preparation of biomorphic wood-based SiC consisted in the carbonization of the wood followed by gas phase

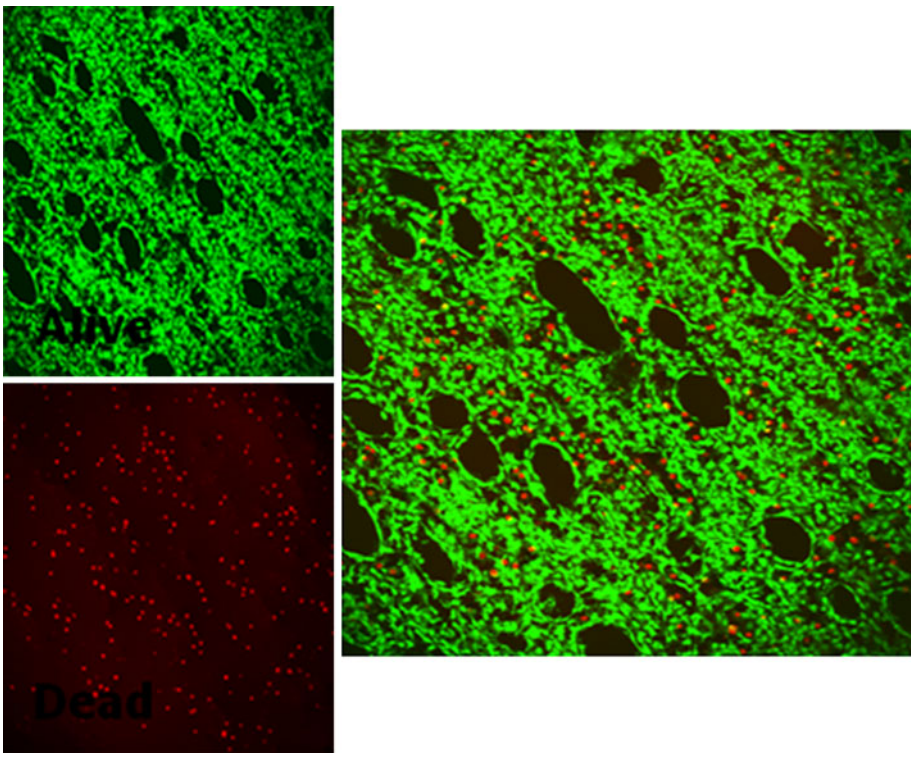

Fig. 4 Calcein-propidium iodure staining observed by confocal microscopy 24 h after seeding on bioSiC samples. Living cells in *green* and dead cells in *red*

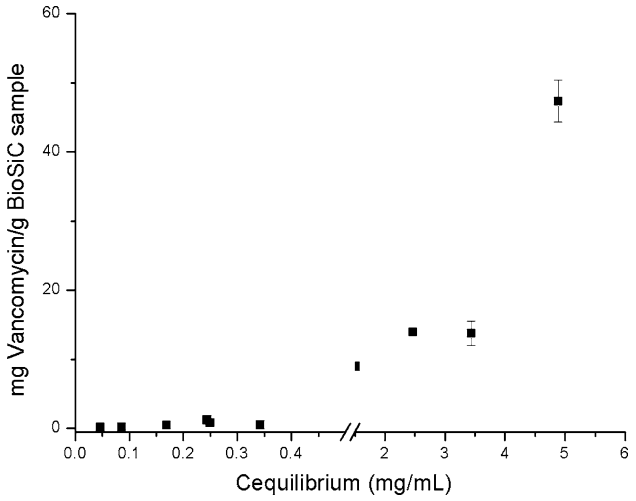

Fig. 5 Vancomycin adsorbed on bioSiC samples (mg/g) versus vancomycin concentration at the equilibrium

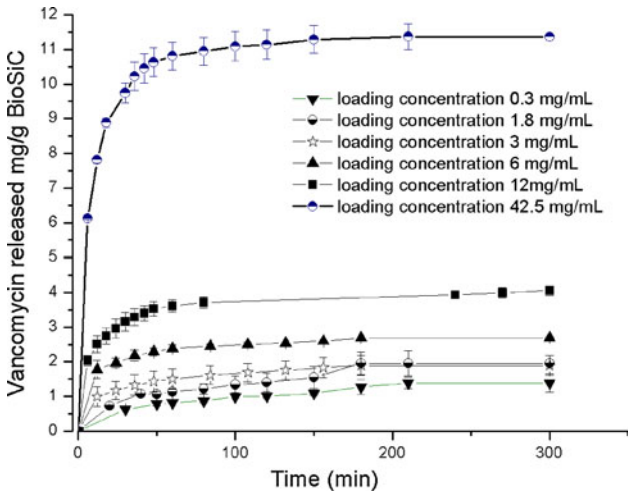

Fig. 6 Vancomycin release from bioSiC samples at the different conditions studied

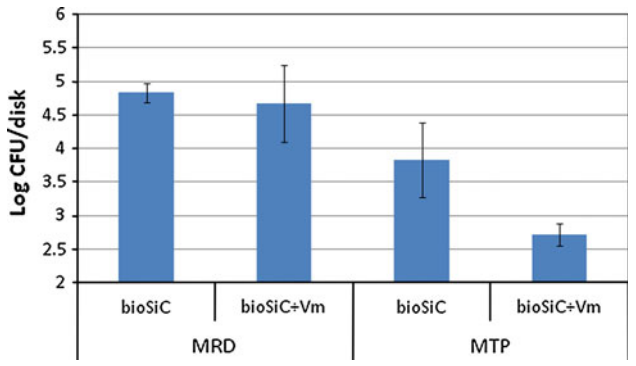

Fig. 7 Log (number of CFU/disk) recovered in both biofilm model systems from bioSiC disks loaded or not with vancomycin. *Error bars* represent standard deviation

infiltration of molten silicon [8]. The resulting structure is expected to have a cellular structure of SiC with elongated silicon channels.

4.1 BioSiC characterization

4.1.1 Morphological characterization

SEM micrographs of bioSiC (Fig. 1) evidenced the particular porous microstructure of the Sapelli tree, with the characteristic groups of two and three macropores (~80 μm), corresponding to vessels (A). The walls of the vessels resisted the reactive molten silicon infiltration resulting in a ceramic material with connected pores. At higher magnifications (B), a second population of mesopores (less than 10 μm) at the surface of the material can be noticed, with the silicon carbide crystals making up the structure both around the pores (B) and inside of them (C). Thus, the particular structure of wood is maintained in the bioSiC [8, 9], resulting in a complex organization with macro and microporosity, both key characteristics for the success of an implant material [1].

Details of the topography and interconnected porosity were obtained by interferometric profilometry. The bioSiC longitudinal section image (Fig. 2a) revealed the presence of long channels over 1 mm completely open and details of the original vascular system. Furthermore, additional information of the topography was obtained by CLSM. The autofluorescence image of bioSiC longitudinal section (Fig. 2b) showed the porous character of the bio-ceramics and the interconnection grade. The fluorescence is emitted by the SiC crystals that constitute the material. Figures 1 and 2 illustrate that the hierarchically-structured vascular system of the vegetal precursor was replicated in the final bioinspired SiC ceramics.

4.1.2 Pore size distribution

To gain insight into the microporous structure, mercury intrusion porosimetry was carried out (Fig. 3). The results indicated a bimodal pore size distribution with macropores (mean diameter 85 μm) and mesopores (mean diameter 3 μm). The total intrusion volume was 0.243 ± 0.005 ml/g and a total porosity of 41.49 ± 0.05%.

Implant microstructure (volume and morphology of the macro and mesopores) has been pointed out as the key issue for the success of a material in surgery [1] as the macroporosity controls the access of the tissues and biological fluids to the volume of the substitute and the microporosity deals with the adhesion of the cells. Moreover, according to current literature, vascularization penetration only occurs when the implant material possesses pores greater than 5 μm and is maximal in pores of 60 μm

[25]. The unidirectional macropores (80 μm, Fig. 1), the presence of a smaller size pore population and their high interconnectivity make the bioSiC from Sapelli potentially able to osteoconduction. Open-pore geometries with highly porous surface and microstructure enable the cell in-growth and reorganization and should provide the necessary space for neovascularization.

It is important to notice that processing variables during bioSiC production may affect the interconnected microstructure of the wood template. Sapelli-based carbons exhibit bimodal distributions derived from its fiber and vessel pores in a range of 0.05–61 μm, which can be partially modified through the infiltration process. In agreement with previous findings due to the volume expansion of ~58% associated with the silicon carbide formation reaction, pores smaller than 1 μm are eliminated [9]. Large pores, on average, also decrease in size due to carbide formation. However in some cases, the pore size distribution shifts towards larger sizes, which can be attributed to the breakage of struts during the expansion reaction, causing some pores to coalesce [9, 26]. These unions could explain the macropores of 85 μm and mesopores of 3 μm found in the pore size distribution of bioSiC from Sapelli.

4.1.3 Density and specific surface determination

The density of the bioSiC disks from Sapelli was 2.9 ± 0.2 g cm^{-3}, which is much higher than the value for pristine Sapelli wood (0.64 g cm^{-3}). According to bibliographic data [13, 27], the density values obtained for bioSiC are closer to that of the cortical bone (1.7–2.0 g cm^{-3}) than other materials currently used in orthopaedics as the cobalt–chromium alloys (8.5 g cm^{-3}) or titanium alloys (4.4 g cm^{-3}). The Sapelli-based bioSiC specific surface was estimated to be 1.198 ± 0.005 m^2 g^{-1}, which is similar to that of commercial bone substitute materials, such as Interpore200® hydroxyapatite (2.64 m^2 g^{-1}), Endobone® hydroxyapatite (0.7 m^2 g^{-1}) or PerioGlass® (bioglass, 0.6 m^2 g^{-1}) [28].

4.2 Cell viability test

The double staining showed that, after 24 h in contact, the cells adhere and grow on the bioSiC surface around the macropores (Fig. 4). The increased fluorescence at the pores edges suggests that cells have colonized the inner surface of the pores. A homogeneously distributed layer of living cells (green) and a significantly smaller amount of dead cells (red) on the top of the bioSiC disks can be observed. The ratio between living and dead cells was used to calculate the viability of cells on the disk. The obtained values were 79.9% (sd 13.1) on bioSiC disks, 98.0% (sd 1.9) on the TCP from the wells and 86.2% (sd 15.3) for the control group. This indicates a good survival of cells on the bioSiC material [29, 30].

4.3 Vancomycin loading

Vacuum was applied to promote the penetration of the drug loading solution into the small pores of bioSiC. Vacuum should remove the air from smaller pores and force the entrance of water along the micropore channels. Adsorption isotherm of vancomycin on bioSiC material enabled to relate the concentration of the solute on the adsorbent (mg vancomycin per gram of dried material) to the concentration of the solute in the surrounding solution at the equilibrium (Fig. 5). A Class S adsorption curve was obtained [22]. This means that, as vancomycin at the outer solution increases, a monolayer of drug molecules is firstly adsorbed on the material and then successive layers of vancomycin can be piled up. This behavior is characteristic of the existence of nonspecific interactions between solute molecules and the adsorbent interface. If the loading were only driven by the equilibration of the drug concentration between the outer solution and the inner aqueous phase of the disks, those disks immersed in 6 mg/ml drug solution could load up to 1.46 mg/g. However, the loading of those disks was nearly 50 mg/g, which confirms the relevance of the adsorption mechanism. The patterning of hydrophobic (e.g. carbon) and hydrophilic (e.g. silicon) regions in the surface of a material, as in the case of SiC, has been previously shown to be favorable for adsorption of DNA and proteins [31]. This may be the case of vancomycin too.

One gram of drug-loaded (50 mg/g) bioSiC immersed in 1 l of medium may provide enough drug to exceed the minimum inhibitory concentration 90% (MIC_{90}) of vancomycin against MRSA (0.25–2 μg/ml [32]).

4.4 Vancomycin release

Drug-loaded disks were immersed in 3 ml phosphate buffer pH 7.4 and no vacuum was applied in order to simulate the release process under physiological conditions. A rapid delivery occurred during the first 2 h, after which the release rate dramatically decreased. In Fig. 6 the profiles for the first hours (critical period after surgery) are shown, but the slow antibiotic release continues for weeks. The total amounts released in the first 2 h are significantly lower but proportional to the adsorbed vancomycin. Since the experiments were carried out under *sink* conditions, this fact may be explained by the difficulty of the medium to access the smaller pores under atmospheric pressure. Thus, the delivery should start from greater pores, acting the small ones as reservoirs for the long term release. The amount of water that penetrates into the disks when no vacuum is applied was measured using a Gay-Lussac

pycnometer. Five minutes after immersion 0.023 ml of water per gram penetrated into the disks. Two hours later the volume of water increased to 0.042 ml, which is less than a quarter of the volume obtained by mercury porosimetry. After 2 h, a progressive but minor increase in the water uptake occurred with time. The initially rapid entrance of water followed by a slower uptake explains the pattern of the vancomycin release profiles.

4.5 Inhibition of MRSA biofilm formation

The effectiveness of bioSiC disks loaded by immersion in 42.5 mg/ml vancomycin solution to prevent MRSA biofilm formation was tested in two model systems (Fig. 7), one (the MRD) in which the growth medium was continuously replaced and another one (the MTP) in which growth medium was not replaced. In the MRD, unloaded control disks contained on average 6.72×10^4 CFU/disk while vancomycin-loaded disks contained 4.61×10^4 CFU/disk, which represents a reduction of 31.4% but not statistically significant. The anti-biofilm effect in the MTP was much more pronounced and statistically significant, meaning a reduction of 92.2%. The more-pronounced anti-biofilm effect in the MTP can be explained by the gradual accumulation of vancomycin over time, while vancomycin is continuously washed away in the MRD model system.

5 Conclusions

BioSiC from Sapelli has a bimodal pore size structure (3 and 85 μm modes) with a total porosity of 41.49% and a density similar to that of the bone. The specific surface area also resembles that of other commercial bone substitutes and enables high vancomycin loading. The combination of different pore sizes enables cell conductive properties and leads to a peculiar drug release pattern with an initially fast delivery (during the critical period for preventing surface colonization) followed by a slower release rate period. The effectiveness of vancomycin-loaded bioSiC against microbial infections was confirmed both under static and dynamic conditions, being able to reduce MRSA biofilm formation. These findings point out bioSiC as a promising biomimetic ceramic from arboreal origin for bone replacement.

Acknowledgments This work was supported by the POCTEP 0330IBEROMARE1P project, FEDER and Xunta de Galicia (PGIDIT07CSA002203PR). The authors acknowledge CACTI (University of Vigo), L. Pereiro-Expósito and L. Balsa (University of Santiago) for the technical support and J. Martínez, A.R. de Arellano-López, F.M. Varela-Feria (University of Sevilla), C. Alvarez-Lorenzo and A. Concheiro (University of Santiago) for helpful contributions.

References

1. Chevalier J, Gremillard L. Ceramics for medical applications: a picture for the next 20 years. J Eur Ceram Soc. 2009;29:1245–55.
2. Huebsch N, Mooney DJ. Inspiration and application in the evolution of biomaterials. Nature. 2009;462:426–32.
3. Weiner S, Wagner HD. The material bone: structure-mechanical function relations. Annu Rev Mater Sci. 1998;28:271–98.
4. Chen QZ, Boccaccini AR. Poly(D, L-lactic acid) coated 45S5 Bioglass®-based scaffolds: processing and characterization. J Biomed Mater Res A. 2006;A-77:445–57.
5. Cui FC, Li Y, Ge J. Self-assembly of mineralized collagen composites. Mater Sci Eng R. 2007;R-57:1–27.
6. Peroglio M, Gremillard L, Chevalier J, Chazeau L, Gauthier C, Hamaide T. Toughening of bio-ceramics scaffolds by polymer coating. J Eur Ceram Soc. 2007;27:2679–85.
7. Vallet-Regi M, Balas F, Colilla M, Manzano M. Bone-regenerative bioceramic implants with drug and protein controlled delivery capability. Prog Solid State Chem. 2008;36:163–91.
8. de Arellano-López AR, Martínez-Fernández J, González P, Dominguez C, Fernández-Quero V, Singh M. Biomorphic SiC: a new engineering ceramic material. Int J Appl Ceram Technol. 2004;1:56–67.
9. González P, Borrajo JP, Serra J, Chiussi S, León B, Martínez-Fernández J, Varela-Feria FM, de Arellano-López AR, de Carlos A, Muñoz FM, López M, Singh M. A new generation of bio-derived ceramic materials for medical applications. J Biomed Mater Res A. 2009;88:807–13.
10. Presas M, Pastor J, LLorca J, de Arellano-López A, Martínez-Fernández J, Sepúlveda R. Mechanical behavior of biomorphic Si/SiC porous composites. Scr Mater. 2005;53:1175–80.
11. Hetrick EM, Schoenfisch MH. Reducing implant related infections: active release strategies. Chem Soc Rev. 2006;35:780–9.
12. Wu P, Grainger W. Drug/device combinations for local drug therapies and infection prophylaxis. Biomaterials. 2006;27:2450–67.
13. Rahaman MN, Yao A, Bal BS, Garino JP, Ries MD. Ceramics for prosthetic hip and knee joint replacement. J Am Ceram Soc. 2007;90:1965–88.
14. Zilberman M, Elsner JJ. Antibiotic-eluting medical devices for various applications. J Control Release. 2008;130:202–15.
15. Teller M, Gopp U, Neumann HG, Kühn KD. Release of gentamicin from bone regenerative materials: an in vitro study. J Biomed Mat Res B Appl Biomater. 2006;81B:23–9.
16. Lepretre S, Chai F, Hornez JC, Vermet G, Neut C, Descamps M, Hildebrand HF, Martel B. Prolonged local antibiotics delivery from hydroxyapatite functionalized with cyclodextrin polymers. Biomaterials. 2009;30:6086–93.
17. Shi X, Wang Y, Varshney RR, Ren L, Zhang F, Wang DA. In vitro osteogenesis of synovium stem cells induced by controlled release of bisphosphate additives from microspherical mesoporous silica composite. Biomaterials. 2009;30:3996–4005.
18. Calhoun JH, Mader JT. Treatment of osteomyelitis with a biodegradable antibiotic implant. Clin Orthop Relat Res. 1997;341:206–14.
19. Gitelis S, Brebach GT. The treatment of chronic osteomyelitis with a biodegradable antibiotic-impregnated implant. J Orthop Surg. 2002;10:53–60.
20. Stanley-Wood NG, Abdelkarim A, Johansson ME, Sadeghnejad G, Osborne N. The variation in, and correlation of, the energetic potential and surface areas powders with degree of uniaxial compaction stress. Powder Technol. 1990;69:16–26.
21. Coenye T, De Prijck K, De Wever B, Nelis HJ. Use of the Modified Robbins Device to study the in vitro biofilm removal efficacy of NitrAdine™, a novel disinfecting formula for the

maintenance of oral medical devices. J Appl Microbiol. 2008;105:733–40.
22. Giles CH, MacEwan TH, Nakhwa SN, Smith D. Studies in adsorption. Part XI. A system of classification of solution adsorption isotherms, and its use in diagnosis of adsorption mechanisms and in measurement of specific surface areas of solids. J Chem Soc. 1960;111:3973–93.
23. Mizutani M, Takase H, Adachi N, Ota T, Daimon K, Hikichi Y. Porous ceramics prepared by mimicking silicified wood. Sci Technol Adv Mater. 2005;6:76–83.
24. Kleist G, Bauch J. Cellular UV microspectrophotometric investigation of Sapelli heartwood (*Entandrophragma cylindricum* Sprague) from natural provenances in Africa. Holzforschung. 2001;55:117–22.
25. Dziubla TD, Lowman AM. Vascularization of PEG-grafted macroporous hydrogel sponges: a three-dimensional in vitro angiogenesis model using human microvascular endothelial cells. J Biomed Mater Res A. 2004;68A:603–14.
26. Pappacena KE, Gentry SP, Wilkes TE, Johnson MT, Xie S, Davis A, Faber KT. Effect of pyrolyzation temperature on wood-derived carbon and silicon carbide. J Eur Ceram Soc. 2009;29: 3069–77.
27. Hallab NJ, Jacobs JJ, Katz JL. Application of materials in medicine, biology, and artificial organs. In: Ratner BD, Hoffman AS, Schoen FJ, Lemons JE, editors. Biomaterials science: an introduction to materials in medicine. 2nd ed. London: Elsevier Academic Press; 2004. p. 532–9.
28. Weibrich G, Trettin R, Gnoth SH, Götz H, Duschner H, Wagner W. Determining the size of the specific surface of bone substitutes with gas adsorption. Mund Kiefer Gesichtschir. 2000;4: 148–52.
29. Neuss S, Apel C, Buttler P, Denecke B, Dhanasingh A, Ding X, Grafahrend D, Groger A, Hemmrich K, Herr A, Jahnen-Dechent W, Mastitskaya S, Perez-Bouza A, Rosewick S, Salber J, Wöltje M, Zenke M. Assessment of stem cell/biomaterial combinations for stem cell-based tissue engineering. Biomaterials. 2008;29: 302–13.
30. Jagur-Grodzinski J. Polymers for tissue engineering, medical devices, and regenerative medicine. Concise general review of recent studies. Polym Adv Technol. 2006;17:395–418.
31. Cicero G, Galli G, Catellani A. Interaction of water molecules with SiC (001) surfaces. J Phys Chem B. 2004;108:16518–24.
32. Rouse MS, Steckelberg JM, Patel R. In vitro activity of ceftobiprole, daptomycin, linezolid and vancomycin against methicillin-resistant staphylococci associated with endocarditis and bone and joint infection. Diagn Microbiol Infect Dis. 2007;58: 363–5.